

## Article

# Ultrasound Sensors for Diaphragm Motion Tracking: An Application In Non-invasive Respiratory Monitoring

Amirhossein Shahshahani <sup>1\*</sup>, Carl Laverdiere <sup>2</sup>, Sharmistha Bhadra <sup>1</sup>, and Zeljko Zilic <sup>1</sup>,

<sup>1</sup> Department of Electrical and Computer Engineering, McGill university, Montreal, Canada;  
{amirhossein.shahshahani, carl.laverdiere}@mail.mcgill.ca,  
{sharmistha.bhadra, zeljko.zilic}@mcgill.ca

<sup>2</sup> Faculty of Medicine, McGill University, Montreal, Canada;  
\* Correspondence: amirhossein.shahshahani@mail.mcgill.ca.

**Abstract:** This paper introduces a novel respiratory detection system based on diaphragm wall motion tracking using an embedded ultrasound sensory system. We assess the utility and accuracy of this method in evaluating diaphragmatic function and its contribution to respiratory workload. The developed system is able to monitor the diaphragm wall activities when the sensor is placed in the zone of apposition (ZOA). This system allows the direct measurements with only one ultrasound PZT5 piezo transducer. The system both generates pulsed ultrasound waves at 2.2 MHz and amplifies reflected echoes. According to the diaphragmatic motions, the respiratory signals of the proposed system is insensitive to human motion artifacts. Promising results were obtained from six subjects on six different tests with an average sensitivity and specificity of 84% and 93% of respiration detection, respectively. Measurements are referenced to a SPR-BTA commercial spirometer. In this study, we also evaluated inertial and photoplethysmography (PPG) sensors as other conventional methods in this area.

**Keywords:** Non-invasive respiratory monitoring; Diaphragm motion monitoring; Breathing disorder; Ultrasound.

## 0. Introduction

High resolution non-invasive monitoring of living organs is essential need as a wearable device or in hospitals for observing physiological activity, mainly the breathing and heart rates [1]. In the intensive care unit (ICU), almost all physiological parameters are measured and monitored, but the assessment of respiratory muscle is lacking [2]. Normal function of the diaphragm is critical for effective ventilation during sleep in normal subjects [3]. Monitoring of respiratory activity is needed to detect respiratory disorders, such as the sleep apnea [4], cessation of breathing in infants [5] or dyspnea. Dyspnea relates to patients having difficulty in breathing, whereas apnea refers to the cessation of airflow during sleep preventing air from entering the lungs. Besides the respiratory rate, depth and patterns are important [6]. The central sleep apnea (CSA) is another form of such diseases in which brain temporarily fails to signal the muscles responsible for controlling breathing [7].

Numerous non-invasive devices for respiration monitoring have been proposed. Appropriate use of current monitoring systems and correct assessment on the provided data are essentials in accurate and trustable diagnosis. Some systems based on direct method are flow meters that use pressure transducers or even thermal and ultrasound flow meters [8] [9], [10]. Aluminum nitride piezoelectric films [11], [12] can measure and monitor the applied pressure on the sensor when a subject is lying on

31 it. The pressure fluctuates on the respiration and heartbeat operations. Another example of a direct  
32 method is chest and abdomen movements analysis using accelerometer sensors [13]. Since the two  
33 later methods are based on the heart beats felt on the skin surface or chest and abdomen circumference  
34 changes due to the breathing, they are sensitive to human motion. Contact-less breathing or heart  
35 rate tracking by low frequency ultrasound sensor is reported by Arlotto et al [14]. This system is  
36 based on radar by detecting the time of flight of ultrasound waves. It can hardly be applied on  
37 different situations and positions, especially when the patient is dressed or covered by a blanket. In  
38 another study, the ultrasound system based on PZT4 piezo transducers were used to monitor heart  
39 and respiration by tracking the motion of heart and its respiratory motions [15].

40 Indirect methods are based on a biofeedback of an organ activity. As an example, photoplethysmography (PPG) sensors measure oxygen level variations due to the breathing [16][17] as well as small blood pressure variations that the pulmonary system applies. They are dependent on many parameters. For instance, the oxygen level depends on oxygen density of the area the person is in [18], bad functions of lungs or airflow, latency between the breathing and oxygen level variations in blood, uncertainty in breath detection at fast respirations and depth of breathing [16]. In addition, it is not favorable to carry a sensor on the finger, earlobe or forehead [19][20].

41 ECG based devices [21] as the most common cardio-respiratory monitoring tools require at least  
42 two conductive electrodes being mounted on chest skin. ECG and PPG devices are the most accurate  
43 and conventional methods in hospitals for heart monitoring, specifically for critically ill patients,  
44 but not ideal for respiratory monitoring. In a study [22], researchers described a signal processing  
45 technique which derives respiratory waveforms from ordinary ECGs, permitting reliable detection  
46 of respiratory efforts. But the data is sensitive to motions and can cause false peaks as a breathing  
47 operation. PPG sensors, as the most popular and inexpensive method for heart rate monitoring, are not  
48 applicable for the direct respiratory monitoring method. It will be explained in more depth in Section  
49 3. Skin conductivity assessment (plethysmography) provides a way to measure respiratory activity by  
50 measuring the thoracic impedance changes caused by inspiration and expiration. Accordingly, this  
51 method requires at least two conductive electrodes which makes it uncomfortable as a wearable or  
52 long time monitoring system. Moreover, the movement-induced artifact on its signal cannot be easily  
53 removed by filtering methods [23][24].

54 Many of the above mentioned conventional techniques are impractical in conditions such as the  
55 patient being fully dressed or under different body position or motion. In a wearable health monitoring  
56 system, it is advantageous if the device monitors while operating under different body positions,  
57 with less constraints on hardware resources and wiring connectivities. In this paper we report an  
58 ultrasound-based organ motion tracking system to extract pulmonary information

59 Ultrasound technology (US) as an inexpensive, safe, and real-time capable that can be used as a  
60 direct method for cardiopulmonary monitoring. Ultrasound imaging systems with an array of piezo  
61 transducers are widely used in diagnosis and imaging [25]. Zambon et al. investigated the use of point  
62 of care ultrasound to assess function of the diaphragm [26], but it involved manual labor and was not  
63 continuous. In this study we used only one sensory node, consists of a PZT-5 piezo disk transducer  
64 as a 1-D tracker of internal organs. A mixed-signal embedded system is designed and operates  
65 in B-mode which generates ultrasound pulses discontinuously and records ultrasound echoes as a  
66 function of intensity and time (depth). By recording the intensity and time of flight (ToF) of reflected  
67 echoes from observing organs, the position of the organ can be found. To determine the velocity and  
68 motion of the organ over time, the system averages the amplitude and depth of specific period of  
69 reflections. This mode is called M-mode and is an analogous to recording a video of ultrasound images  
70 focused on a specific area of images. This technique is widely used in ultrasound imaging for real-time  
71 measurements of heart rate, wall thickness and the thickness abnormality detection [27]. In this paper,  
72 the data from the proposed ultrasound system is evaluated and validated against a spirometer as a  
73 main reference. The data is collected on subjects having no specific illness to do a system validation  
74 and performance evaluation.

## 81 1. Methods and Principles

### 82 1.1. Basics of ultrasound and sensor description

83 As mentioned before, the proposed system is based on ultrasound technique. The transducer  
 84 used in the sensor is a 2.2 MHz PZT5 piezo disk operating in thickness mode. One main issue in piezo  
 85 disk transducers operating at frequencies higher than 1 MHz is the transducer's electrode connectivity.  
 86 One side of the sensor has to be interfaced with a acoustic matching layer, with the overall thickness  
 87 of  $\lambda/4$  [28], while having an electrical conductivity to the circuit.  $\lambda$  is the acoustic wavelength in the  
 88 propagation medium which is discussed in the following. Since the other side of sensor is covered by  
 89 a backing layer or left open as an air-coupled backing, the connectivity in this side is not a problem.  
 90 Hence, the piezo transducer is mounted by a silver epoxy on a Kapton (polyimide) film, 125  $\mu m$   
 91 thickness. We printed a silver conductive pad (flexible silver conductive ink) on this film to connect  
 92 the transducer's electrode to the rest of the sensor circuit using VOLTERA circuit printer. The printed  
 93 substrate and finalized design is shown in Fig. 1. Having silver as the main component of this epoxy,  
 94 printed ink and transducer's electrode results in a good acoustic impedance matching between the  
 95 transducer and the printed circuit layer.

96 To remove air gaps between the sensor and skin, only a conductive soft material, such as  
 97 ultrasound gel, is needed to be rubbed on the skin surface. There are many alternatives, such as  
 98 water, baby oil or hand cream which have almost equal performance and the patient is not limited to  
 99 use the ultrasound gel. The conductive medium enables a tight bond between the skin and the sensor,  
 100 letting wave transmissions directly to the tissues underneath. With only a pair of wire connection,  
 101 the proposed system lessens the number of connected electrodes or sensors directly to the skin. One  
 102 strap band or an adhesive pad is needed to hold the sensory head on its position. However, the  
 103 adhesive pad will ensure the sensor's position and lessens the motion artifact of signals. In soft tissues,  
 104 about 80% of the ultrasound wave is absorbed by the tissue resulting in local heat production on cells  
 105 [29]. Acoustic impedances and attenuation coefficients of some specific mediums and soft tissues  
 are listed in Table 1. Ultrasound waves are attenuated in a medium with higher value of attenuation

Table 1. Acoustic Properties of Biological Tissues

Medium	Attenuation Coefficient (dB/cm)	Acoustic Impedance (kg/m <sup>2</sup> .s or rayl)*10 <sup>6</sup>
Water	0.002	1.48
Blood	0.18	1.61
Fat	0.63	1.38
Muscle	1.3-3.3	1.62
Bone	5.0	6.0
Silver	16	5.14
Ultrasound Gel	-	1.6

106 coefficient. In the human body, bone has the highest attenuation coefficient which hardly allows beam  
 107 transmission through itself. In addition, due to the high acoustic impedance mismatch between bone  
 108 and tissues, intensity of reflections are high. Small upper body motions do not impact the ultrasound  
 109 wave propagation and these waves can still pass through the gap between rib cage bones. Big skin  
 110 movements may result in a noticeable sensor displacement and ultrasound wave blockage if the sensor  
 111 faces the bones. This misplacement leads to an error in reading ultrasound reflection. Such a big  
 112 displacements rarely happen when the patient is not in intense motions.

114 Vibration (resonant) modes of piezo-ceramic transducers depend on their shape, polarization  
 115 orientation and the direction of the electric field. The acoustic axial resolution of the sensor can  
 116 be calculated as below by considering the average sound velocity of tissue as  $c = 1540m/s$  and

<sup>117</sup>  $f = 2.2\text{MHz}$  used in this study:

<sup>118</sup>

Axial Resolution:

$$\theta_z = \frac{\lambda}{2} = \frac{c}{2f} = \frac{1540(\text{m/s})}{2 * 2.2 * 10^6} \simeq 0.35 \text{ mm} \quad (1)$$

<sup>119</sup> K. M. Langen *et al.* [30] summarized evaluations on diaphragm motion studies. The average  
<sup>120</sup> peak-to-trough (PTT) diaphragm movements measured 13 mm in normal breathing and 39 mm during  
<sup>121</sup> deep breathing. Hence, the axial resolution of 0.35mm should provide an adequate accuracy to measure  
<sup>122</sup> the internal organ motions. The accuracy of the measurements at higher frequencies improves but the  
<sup>123</sup> power consumption and system complexity increase accordingly while the depth of ultrasound wave  
<sup>124</sup> penetration decreases proportionally.

<sup>125</sup> 1.2. *Sensor Position*

<sup>126</sup> In this study, the goal is to investigate the motion of the diaphragm, thus the sensor was positioned  
<sup>127</sup> in the zone of apposition (ZOA). The ZOA is the area of the diaphragm encompassing the cylindrical  
<sup>128</sup> portion (the part of the muscle shaped like a dome/umbrella) which corresponds to the portion directly  
<sup>129</sup> apposed to the inner aspect of the lower rib cage [31]. The piezo sensor is placed on the right, as it is  
<sup>130</sup> easier to see the diaphragm with the liver window [32]. Following methods described in the literature  
<sup>131</sup> [26],[33],[34],[35], the sensor was placed between ribs 8<sup>th</sup> and 9<sup>th</sup> at the mid-axillary line (Figure 1).  
<sup>132</sup> Having the sensor positioned in this zone will enable it to see both contraction and relaxation of the  
<sup>133</sup> diaphragm. The diaphragm is an hyperechoic structure, which means that ultrasound can be reflected  
<sup>134</sup> and measured [32]. Although it is behind the thoracic rib cage, its motion can be seen by ultrasound  
<sup>135</sup> from the intercostal space.

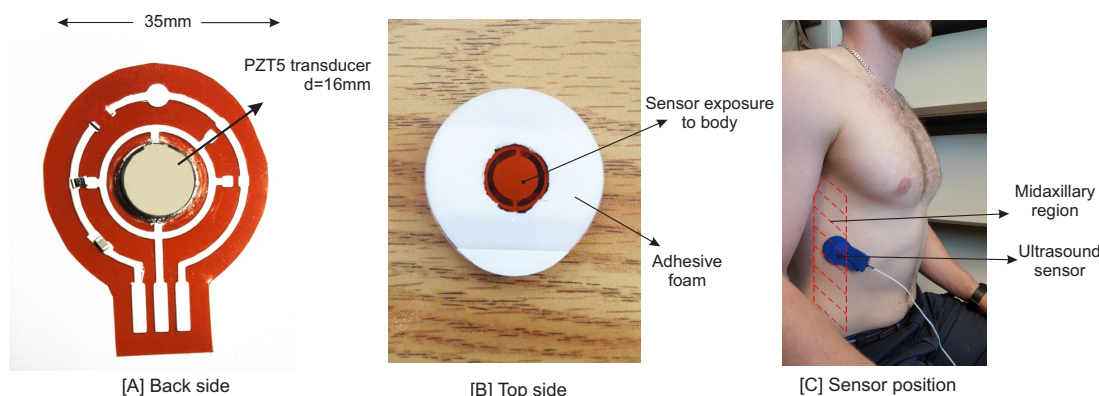


**Figure 1.** (A) The PZT5 piezo transducer mounted on a flexible printed PCB circuit. (B) The top side of sensor. A two-sided adhesive pad is used to hold the sensor on the body. The middle round area is filled by ultrasound gel. (C) Sensor position in the zone of apposition (ZOA). The sensor on back side is covered by a blue tape.

<sup>136</sup> 1.3. *Study Protocol*

<sup>137</sup> As discussed, we are monitoring the internal organ motions, mainly the diaphragm wall. Our  
<sup>138</sup> goal is the evaluation of the proposed system on subjects having different body sizes. Four practical  
<sup>139</sup> tests are done in resting state to ensure an accurate assessment versus the references explained in  
<sup>140</sup> the following. Moreover, two additional tests are done when the subject had upper body motions to  
<sup>141</sup> examine the system under the human motion artifact. All tests were done in a sitting position. Tests  
<sup>142</sup> are detailed as following:

- 143 • Test-T1, Normal breathing: In this test the subject was asked to ignore the apparatus and breath  
144 normally.
- 145 • Test-T2, Normal breathing with two breath holds: In this test the subject starts with two or three  
146 normal breaths and then a long inhalation followed by a long exhalation. This test is done to  
147 evaluate the system on breath holds, or when the subject is in suffocation.
- 148 • Test-T3, Fast breathing: In this test, the subject breaths fast (between 25 and 40 breathing cycles  
149 per minute) like a real situation after an exercise.
- 150 • Test-T4, Normal and weak breathing: This test is a simulation of real situation which the subject  
151 is in a rest and breaths gently.
- 152 • Test-T5, Normal breathing with hand elevation: This test is intended to evaluate the skin  
153 movements when the subject abduct his arm up to shoulders and then completely up. As  
154 mentioned before, if the sensor is placed in front of a bone, then the measurements are impossible  
155 due to the ultrasound wave blockage.
- 156 • Test-T6, Breathing with upper body motions and rotations: In this test the subject is asked to  
157 move his/her upper body randomly in all directions. This is to show and proof the merit of this  
158 system being fairly insensitive on upper body motions.

#### 159 1.4. Ethics Approval

160 All participated subjects gave their informed consent which was approved by the appropriate  
161 ethics committee (Research Ethics Board II Office, McGill university, approval number 252-1117). There  
162 are no known risks associated with the experiments on subjects asked to perform. In some cases it  
163 caused dry mouth which was eliminated by providing enough rest interval between each breathing  
164 patterns and drinking water. Moreover, Ultrasound has been shown on many occasions to be safe  
165 when the acoustic waves are under threshold [36]. In a study, a similar sensor was evaluated to prove  
166 the amount of ultrasound wave intensities being less than the threshold values [37].

#### 167 1.5. Validation process

168 To validate the data obtained from ultrasound system, a reference from which the breathing rate  
169 and the intensity can be calculated accurately is needed. Spirometer and plethysmography based  
170 devices are most known clinical and commercial references. We used a SPR-BTA spirometer with  
171 GO!Link data logger software to measure oral breathing in rest condition. A nose clip is used to  
172 prevent nasal breathing. This device measures the amount of airflow not the volume. Accordingly, the  
173 signal level returns to zero in breath holds. Since the proposed measurement method is a based on the  
174 volume of air the subject inhales or exhales, trapezoidal numerical integration is used to compute the  
175 approximate integral of the signal.

## 176 2. System Architecture

177 Fig. 2 shows the block diagram of the system designed and implemented to extract, record and  
178 monitor the ultrasound data, and validate it against the references. The digital and analog subsystems  
179 are employed; the analog sub-system has two main paths: a transmitter (TX) and a receiver (RX). A  
180 commercial IC MAX-14808 is deployed as the front-end high voltage (HV) pulser, switch and damper  
181 in a single chip. It hence acts as the transmitter and path separator. Also, this IC is a High Voltage  
182 (HV) Pulser used to generate a differential pulses up to  $\pm 20$  volt to increase the intensity of ultrasound  
183 waves. We employ the pulser in three main operation modes, controlled by two signals. First, the  
184 differential HV pulses are applied to the transducer and after 5 to 10 pulses, the voltage returns to zero  
185 and then the damper turns on for a short time to diminish the ringing effect and possibly stored high  
186 voltage charges. In the third step, once the internal switch is connected to the RX path, the receiver  
187 circuit amplifies the low voltage reflections from sensor.

188 A two-stage linear amplifier with a wide passive band-pass filter magnifies reflected ultrasound  
189 beams from undesired high and low frequency components of the signal. The magnified signal is

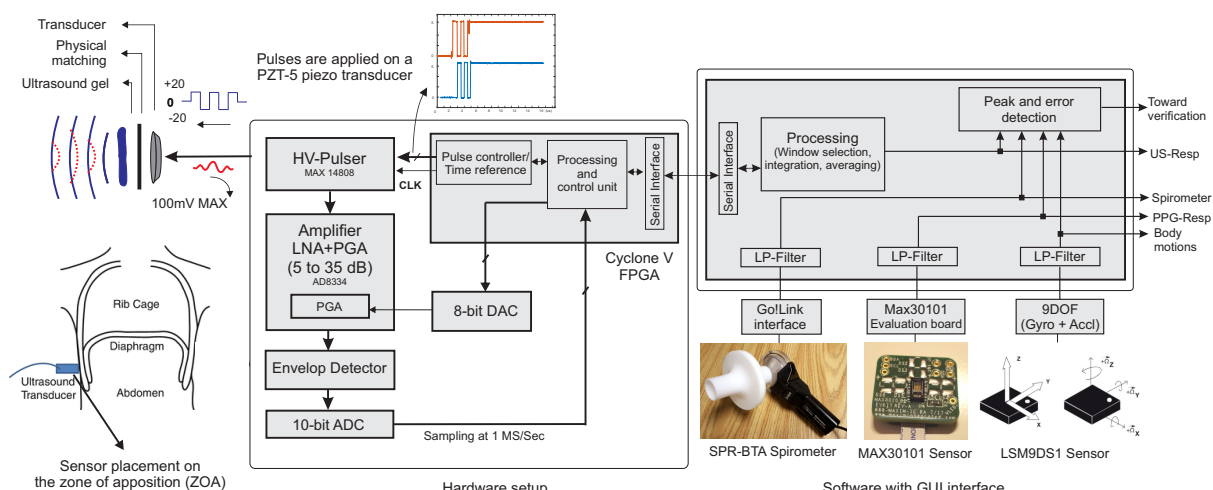


**Figure 2.** Ultrasound system designed to continuously measure and monitor respiratory cycles. Spirometer and PPG sensors are used as references for ultrasound data validation.

passed to an envelope detector which helps to reduce the digital signal processing work. It is worth noting that the energy of ultrasound waves attenuates as it moves through tissues. The amplitude decreases approximately by 1 dB per 1 MHz per 1 centimeter traveled [28], so our ultrasound wave weakens by 1 dB for each centimeter of tissue penetration. To increase the sense of reflections from deeper tissues, the gain of amplifier should increases linearly with the same ratio as the ultrasound waves attenuates. For this purpose, an analog front end (AFE) designed with an integrated low noise amplifier (LNA) followed by a variable gain amplifier (VGA). The gain is controlled by an analog voltage generated by an 8-bit digital to analog converter (DAC). Once the switch turns to RX path, the gain starts increasing from 10 to almost 30dB within 200 us. This time is chosen as it is the maximum period during which we expect to have the reflections. Finally, since the information of each echo is carried on the amplitude and flying time of reflections, the envelope of the signal is extracted. The envelope can be produced in analog circuit with a simple rectifier and low pass filter or using Hilbert transform with the digitized values. The Hilbert transform method exhibits better performance, as it detects the true amplitude of the analytic signal. However, the analog subsystem will reduce the required ADC clock and processing units dramatically since the carrier frequency is removed.

To digitize the enveloped signal, we used an 8-bit resolution analog to digital converter (ADC) with the sampling frequency of 1Ms/s. It converts the analog signal once the system switches to RX mode for 200 samples (lasting 200 us).

A Cyclone V FPGA programmable logic device is programmed to control all blocks through digital pulses. The data is logged and processed by MATLAB (Matrix Laboratory, USA) with a user-friendly GUI interface. The processing on ultrasound data can be done completely on the FPGA. However, to make a better timing comparison between all three resources, processing is done on the computer for the purpose of our experiments.

The hardware setup of the proposed system architecture is shown in Fig 3. The proposed system requires +3.3 voltage sources for the digital and analog integrated circuits and the differential  $\pm 5$  to  $\pm 20$  volts from an external DC linear power supply for the transducer stimulation. It consumes 34 mA for the digital and analog circuit. The transducer itself consumes less than 0.1 mA on different voltages. Only 393 logical blocks of a Cyclone II FPGA are used.

### 2.1. Pulse Generation and Observation

The average intensity of acoustic waves depends on pulse repetition factor and the voltage level. As the voltage applied on the transducer increases, the intensity of acoustic waves increases as well.

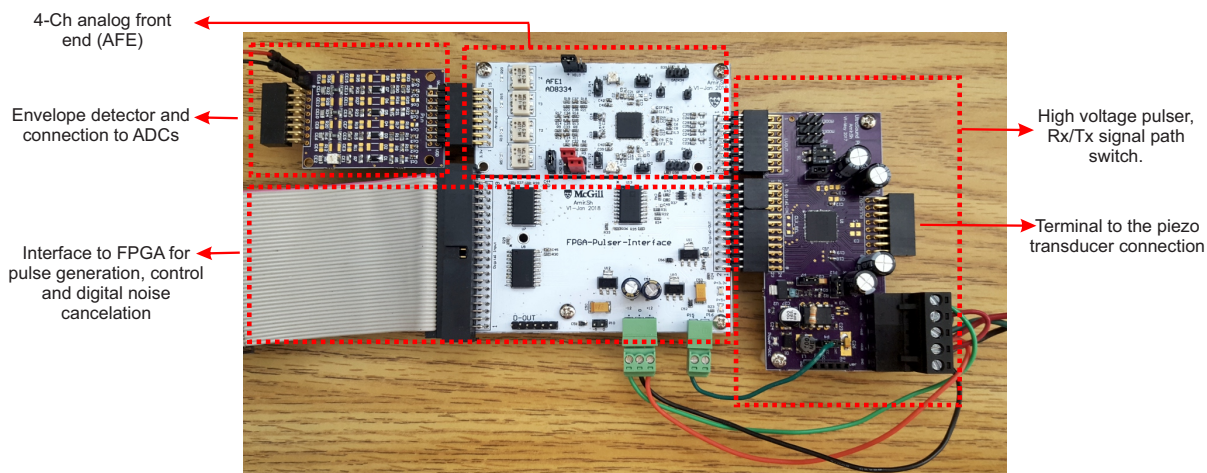


**Figure 3.** The designed 4-channel ultrasound system hardware setup consists of high voltage pulser, analog front end (AFE), envelop detector and ADC. It is interfaced to a Cyclone V FPGA board as a controller and data logger to the computer.

221 And, as the repetition factor increases, the refreshment of these information increases as well. In this  
 222 study, we are planning to measure the near tissue movements, meaning low energy acoustic pulses are  
 223 sufficient to stimulate the transducer. In this study, we examined our system by pulses on differential  
 224 voltages from  $\pm 5V$  to  $\pm 20V$  applied on the transducer. Observations and measurements have shown  
 225 that even  $\pm 5$  voltage rating is sufficient for the diaphragm motion tracking. Monitoring of subjects  
 226 with thicker skin, fat and rib cage may require higher acoustic energies as the depth of penetration  
 227 increases. Operation in lower voltages also consumes less energy and applies weaker ultrasound  
 228 wave intensities, which might have the inappreciable side-effects on the body. However, ultrasound is  
 229 known for its excellent safety record.

230 Fig. 4 shows an example of received waveforms when the sensor is placed on the ZOA. The blue  
 231 and orange waveforms in Fig. 4.A are two examples of the envelope of echoed signals received in  
 232 inhalation and exhalation, respectively. The required information lies under the peaks amplitude and  
 233 their locations (ToF). The largest peaks marked on this figure at times less than about 20  $\mu$ s are a result  
 234 of sensor's ringing effect and reflections from unmatched surfaces, from sensor to skin surfaces.

235 Fig. 4.B depicts a one minute of *Records* for a subject in rest without body movements to monitor  
 236 the diaphragm wall motions. This 3000 records is a series of the envelope signals, such as one shown in  
 237 Fig. 4.B, recorded at every 20 ms. Results are similar to M-Mode ultrasound imaging where M stands  
 238 for motion tracking over time.

In this test, the subject started with three normal breathing. After that, two breath-holds (with full inhalation and exhalation), followed by normal breathing cycles continued to the end. In this figure, the amplitude variations of each record contains the respiration information. Since these peaks are results of an internal organ motion, rather than external motion or skin surface, the obtained information is shown to be robust to the human motions. Additionally, the monitoring is based on a direct measurement of a physiological human activity, and not by an indirect method. To obtain the respiratory waveform, the integral of the signal or the mean value within the *desired window* of each record gives a value ( $M_j$ ). This is the period of time the ultrasound reflections from the desired internal organs receive. Reflections before this period are results of motion artifact, sensor ringing

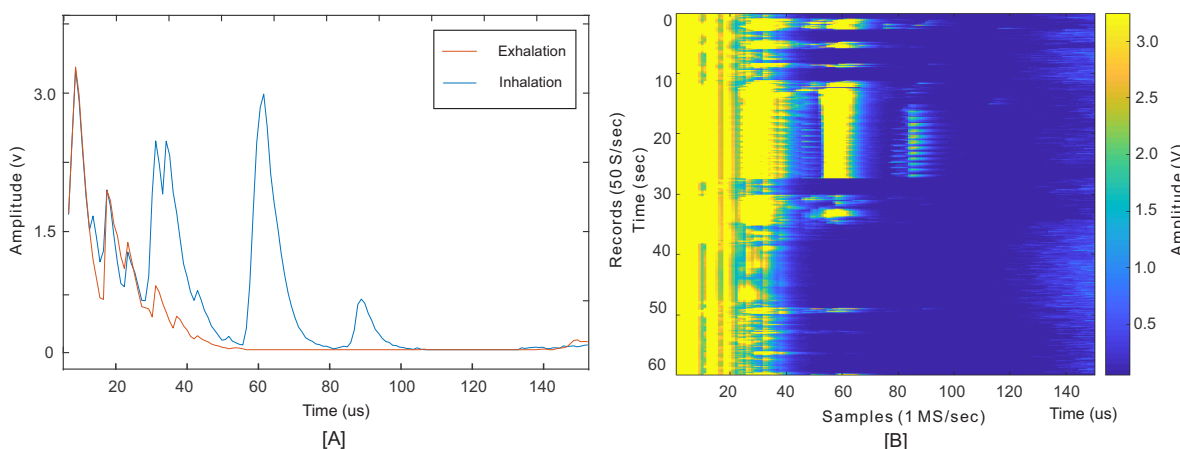


**Figure 4.** (A) An example of obtained signal sampled at 1 Ms/sec at the end of each inhalation and exhalation, each called a *Record*. (B) A one minute of *Records* taken at 50 Hz depicts the breathing cycles.

effect and small spikes from the internal switch when it turns into RX mode. For this study, the period is set from the time 22 to 100 us, so ( $M_j$ ) can be found as:

$$M_j = \frac{1}{UB - LB} \sum_{i=LB}^{UB} S_{ji} \quad (2)$$

where  $j$  and  $i$  are the *record* and *sample* indices, respectively (on axes Y and X). The LB and UB are the lower and upper bounds of the *desired window*, as explained above. A series of  $M_j$  values for all records produces a signal shown in Fig. 5 as US (ultrasound). A low-pass FIR filter is used to emit high frequency elements of the raw signal, which is higher than 1 Hz. Same filters are used to apply on signals from the spirometer, the PPG and motion sensors. FIR filters of the same order (order 12) are used for filtering to ensure linearity in phase of filtered data which is an important criterion for filter selection, especially for validation procedure.

### 3. Results

For all the listed tests, the inertial sensor is placed on the ultrasound sensor to monitor the body motions and motions due to the breathing. This sensor provides 3 axis accelerometer and gyroscope data at the same data rate as ultrasound. We used MAX30101 multi-sensory board, which provides a proven design to evaluate the integrated pulse-oximetry and heart rate monitoring. PPG sensor is selected as a comparative technique to the proposed ultrasound system. Some studies proposed the use of PPG sensors for respiration estimation as discussed in the Introduction. But, to the best knowledge of the authors of this article, there is no evident or practical test on respiratory monitoring when the breathing is fast or the subject is moving. In this study, we evaluate the PPG under the same conditions as our proposed system.

Figures 5 and 6 show the signals of our ultrasound system (US), PPG, spirometer and motion sensors for a minute record, as measured on a subject. It helps to compare waveforms visually and have better assessments on the proposed system functionalities. Tests T1, T2, T3 and T4 in Fig. 5 are experiments without body motions and the T5 and T6 tests in Fig. 6 are designed to evaluate the system under body motions. Our observations and analysis on the PPG data when the subject was moving showed uncertainty in the respiratory waveforms. Therefore, we skipped showing the PPG data for tests T5 and T6. Instead, the accelerometer data is added to show the position of the body.

263 Among the gyroscope and accelerometer sensors data, the gyroscope was found to produce a  
264 better signal. Although the magnitude of data from these two sensors is extremely small, gyroscope  
265 signal is still more detectable than the accelerometer data.

266 *3.1. Ultrasound Data Validation - static body posture*

267 The Test T1 in Figure 5 consists of 16 normal inhalations and exhalations per minute. As evident  
268 in this figure, the ultrasound system (US) has a clear breathing detection versus the reference (ESP).  
269 The PPG sensor's data follows the respiratory waveform with a lower accuracy and intensity while  
270 the gyroscope data has peaks which could be counted as wrong detections.

271 Test T2 is a normal breathing with two breath holds. In this test, all subjects begin with three  
272 normal breathings. Then, they were asked for twice to hold their inhaled breaths for 10 to 20 seconds  
273 followed by an exhalation. It continued with normal breathing to the end after the breath-holds. This  
274 test was done to simulate the apnea situation and feasibility of an apnea detection using the proposed  
275 respiratory monitoring. According to the signals of this test in Fig. 5, not only the PPG sensor did not  
276 follow the overall breathing patterns, except the three true detections in the beginning, but also peak  
277 signals generated by this sensor could be realized as breathing activities. The gyroscope could provide  
278 a better signal than the PPG, however the sensor generated some peaks at the end which could be  
279 counted as breathing. In addition to the breathing operation detection, the system is able to show the  
280 diaphragm efforts when applying pressure to open the airway. In a study by Holland et al. [38], they  
281 showed that breath holding does not eliminate motion of the diaphragm and the diaphragm moves  
282 upward during a breath hold with a constant velocity of 0.15 mm/sec. This phenomenon is evident in  
283 our data shown in Fig. 5 US of Test T2. The mean amplitude of the signal lowers almost constantly by  
284 the time. Understanding this biofeedback would help analysis to distinguish the apnea, while other  
285 methods such as motion tracking sensors may consider any static respiratory signal as an apnea.

286 Test T3 is the same as Test T1 except that the breathing is faster. This test is done not only to  
287 evaluate the performance of the proposed system but also the PPG response to the fast breathing. Our  
288 analysis shows a weak correlation and breath detection of PPG sensor versus the reference and good  
289 responses of the Gyro and ultrasound system. Almost 4 breaths were not detected by the ultrasound  
290 system. Detailed results are listed in the Table 2 and 3.

291 Test T4 is done with the same goal as Test T3 to compare the two PPG and US sensors versus  
292 the reference. The subject began with the shallow breathing for almost 30 seconds and continues  
293 the normal breathing to the end. Our US signal could detect the weak breathing functions but the  
294 amplitude of changes was as low as the motion sensor, while PPG sensor did not provide any relevant  
295 signal to the weak breathing. All sensors operated well in normal breathing for the rest of 30 seconds. It  
296 is worth noting that the US system did not generate false readings as the Gyro and PPG did, specifically  
297 evident in the first 30 seconds.

298 *3.2. Ultrasound Data Validation - dynamic body posture*

299 The proposed system assessments versus other methods under upper body motions are shown in  
300 Fig. 6. We practiced Test T5 to evaluate the sensor displacement and its consequence on respiratory  
301 data. In this test, the subject started with two normal breaths and then abducted his right arm up to  
302 90 degree for two more breaths in this position. Then abducted more up to 150 degree and breathed  
303 two times again. Finally, he continued breathing when brought the hand to the mid and then initial  
304 position. The right hand was chosen because the sensor was placed on the right ZOA area. The skin  
305 around the ZOA shifted vertically by hand elevation. This shift caused the sensor to be placed in front  
306 of the rib cage bones. Our analysis on subjects showed that the system operated ideally as long the  
307 elevation is up to the 90 degree. The system failed to detect respiration operation on Half of subject  
308 tests when the hand was elevated more than 90 degree.

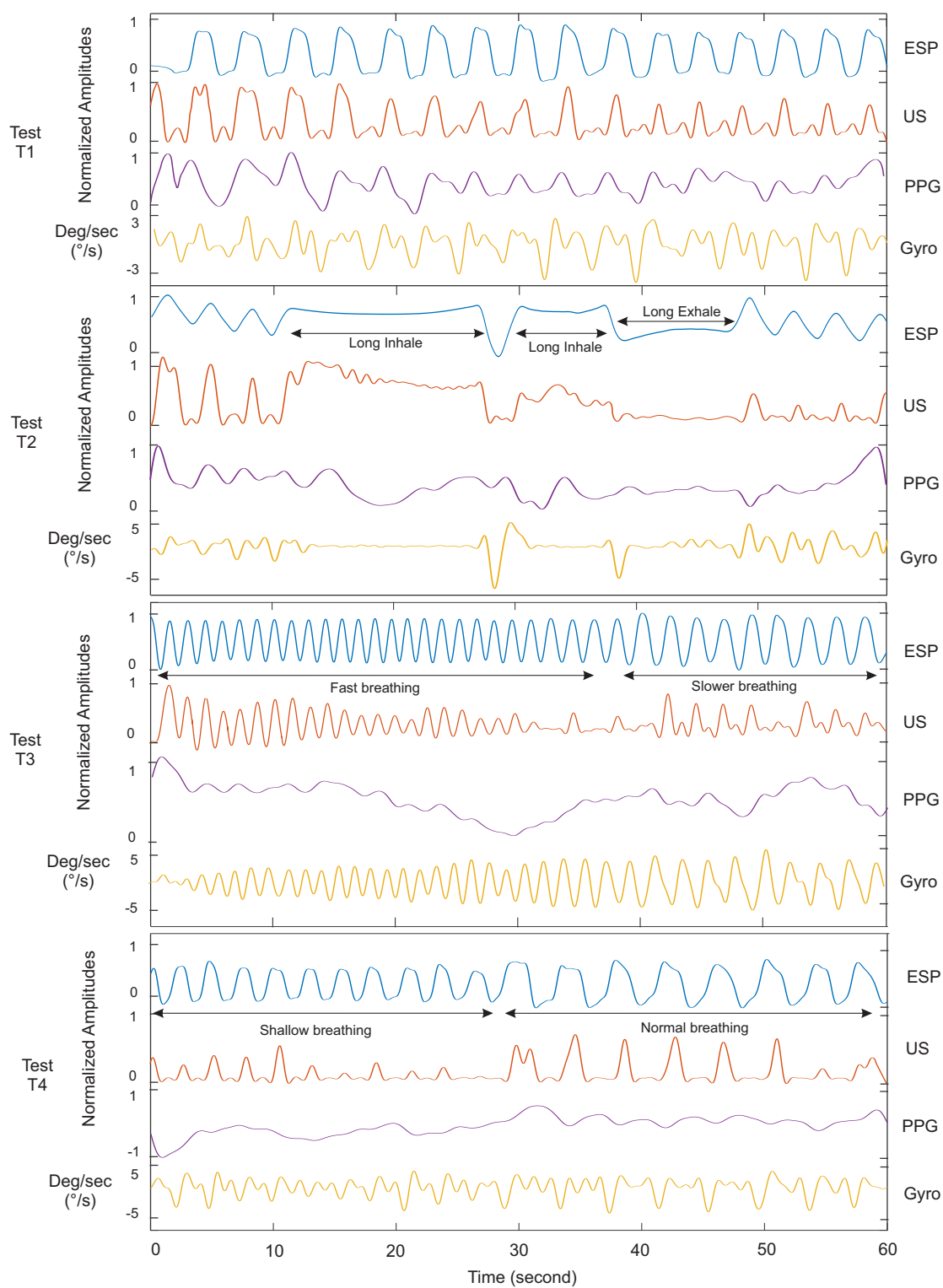


**Figure 5.** Respiratory waveforms of the proposed ultrasound system (US) in comparison with spirometer (ESP), pulse oximeter (PPG) and motion sensor (Accl/Gyro). Only four out of six types of experiments are plotted in static body conditions. All tests are in close resemblance to real breathing situations.

Finally in the Test T6, the proposed method was examined by upper body motions. An example of this test is shown in Fig. 6 while the subject bended to left and right within 25 seconds, and then was almost in gentle motions for 10 seconds. The subject continued to the end by fast and big motions while was breathing normally. Analytical results and observations showed a fairly correlated data versus the reference when the subject's body had motions, but the sensor displacement on the first 25 seconds did not allow the system to track the diaphragm's movements (the similar issue in Test T5). Due to the hand and body motions, the PPG data collection was skipped in these two tests as this sensor is sensitive to motion artifacts.

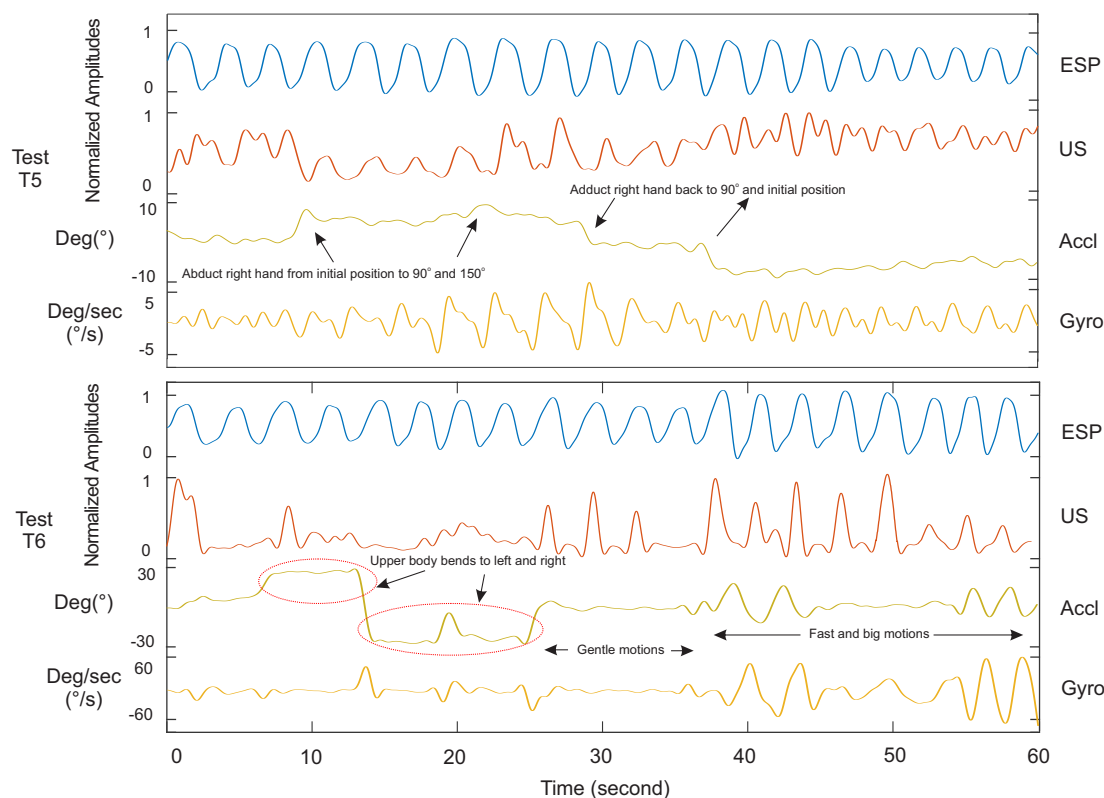


**Figure 6.** Respiratory waveforms of the proposed ultrasound system (US) in comparison with spirometer (ESP) and motion sensor (Accl/Gyro). Since the PPG data is sensitive to the sensor motion, its signal is skipped for presentation and analysis in T5 and T6.

Table 2 is a list of sensitivity, specificity and precision evaluations of all methods with regard to the reference. The sensitivity or true positive rate (TPR) is calculated by the equation below:

$$Sensitivity(TPR) = \frac{TP}{TP + FN} \quad (3)$$

In this equation, the true positive (TP) is the number of correctly detected full breathing operations and false negative (FN) is the number breaths wrongly classified as negative. In this table, the total number of breaths per minute of the spirometer is listed. The specificity or the true negative rate is calculated to identify the proportion of non-breathings that are correctly identified, and can be calculated using below equation:

$$Specificity(SPC) = \frac{TN}{TN + FP} \quad (4)$$

In addition to sensitivity, precision or positive predictive value (PPV) is calculated by Eq. 5. In this equation, the false positive (FP) is the total number of breathing operations detected by an error. This

**Table 2.** Statistical measurements of all experimental tests on 6 subjects. Results are compared with the spirometer as a reference. The average number of breaths per minute of all tests are measured by spirometer. As shown in Fig. 5T5 and T6, the inertial and PPG sensors are not applicable (NA) for respiratory monitoring when the subject's body moves.

Test number	Breaths per minute	Sensitivity (%)				Specificity (%)				Precision (%)			
		US	Accl	Gyro	PPG	US	Accl	Gyro	PPG	US	Accl	Gyro	PPG
Test1	13	86	73	81	68	98	91	79	92	98	84	75	88
Test2	11	89	78	86	48	98	88	75	86	98	88	76	84
Test3	25	87	63	94	27	92	84	90	85	92	81	90	77
Test4	16	89	81	84	59	91	93	80	94	88	90	79	95
Test5	16	78	71	87	N/A	94	81	73	N/A	94	86	74	N/A
Test6	17	73	N/A	N/A	N/A	89	N/A	N/A	N/A	89	N/A	N/A	N/A
Average	N/A	84	73	86	51	93	86	79	86	94	87	79	89

326 error in ultrasound system could be a result of sensor displacement which rarely happened during  
 327 our experiments. This value is noticeably high for the gyroscope. The statistics of the Test T6 are not  
 328 calculated for the gyroscope, accelerometer and PPG sensors due to the extremely noisy and useless  
 329 data.

$$Precision(PPV) = \frac{TP}{TP + FP} \quad (5)$$

**Table 3.** Summary of subjects specifications. CC is the chest circumference.

ID	Age (year)	Height(cm)	Weight (Kg)	CC (cm)
1	36	173	73	84
2	29	176	65	81
3	26	175	75	84
4	25	183	95	88
5	27	165	50	74
6	34	175	70	74

330 According to the above mentioned results and visual observations, the author did not find a  
 331 relationship between the body specification and system performance. Observations showed that  
 332 subjects having more fat in the zone of apposition have more difficulty to find a right place for sensor  
 333 position. As explain before, the sensor has to be placed between ribs. So, a thicker or softer skin results  
 334 more sensor displacement than thinner or skinny body.

### 335 3.3. Non-respiratory movements

336 As mentioned before regarding the *desired window*, the system looks into reflected ultrasound  
 337 waves from internal organs, mainly the diaphragm. Among all the subject tests of T6 in this article,  
 338 none of the tests showed any correlation with body motion. In some tests where the subject held  
 339 the breath for a longer time, there were some small peaks in the signal due to the heart operation.  
 340 Heart contractions transmit motions to the surrounded organs, such as the pericardium sac and the  
 341 diaphragm.

## 342 4. Discussion

343 Based on observations over all experiments, a weak correlation is found between the PPG  
 344 and spirometer respiratory waveforms. As per the discussion on indirect methods for respiratory  
 345 monitoring systems in the introduction, the PPG sensor responds slowly to the oxygen level variations  
 346 in blood. In fast breathing, the PPG response is weak compared to a reference such as spirometer and

347 the proposed ultrasound system, as plotted in Fig. 5. In addition, the application of the PPG sensor as  
348 a respiratory monitoring device is extremely sensitive to motion artifacts.

349 The proposed ultrasound system provides a robust respiratory signal using only one sensor  
350 placed in the zone of apposition. Although the system is sensitive to sensor displacement, it does  
351 not generate false detection when compared to the other methods. To improve the displacement  
352 sensitivity, an array of transducers enables the system to track the diaphragm motions by at least one  
353 transducer even if others are blocked by the ribs. An array of 3 transducers placed side by side within  
354 the intercostal space could be a solution to overcome this issue. Note that transducers are placed on a  
355 flexible material and are not causing any discomfort nor inconvenience for the subjects.

## 356 5. Conclusions

357 In this paper, we presented an accurate and direct respiration monitoring system based on pulsed  
358 ultrasound technique. The sensor consists of a PZT5 piezo transducer mounted on a flexible surface  
359 being in contact to the skin surface. The sensor should be placed on the zone of apposition (ZOA) on  
360 the right side of body to observe the motion of diaphragm. The proposed diaphragm motion tracking  
361 sensor provides fairly good detection of respiratory cycles, according to the nature of the applied  
362 technique in which the systems looks into an internal organ motions not the external or surface motions  
363 of the body. The system was examined by a spirometer as the main reference. In addition, an inertial  
364 and photoplethysmography (PPG) sensors are employed to evaluate their operation according to the  
365 reference and our proposed technique. Our ultrasound sensor was robust to upper body motions in  
366 comparison to the inertial and PPG as two conventional methods for respiratory monitoring.

367

- 368 1. Vivier, E.; Dessap, A.M.; Dimassi, S.; Vargas, F.; Lyazidi, A.; Thille, A.W.; Brochard, L. Diaphragm  
369 ultrasonography to estimate the work of breathing during non-invasive ventilation. *Intensive care medicine*  
370 **2012**, *38*, 796–803.
- 371 2. Sigala, I.; Vassilakopoulos, T. Diaphragmatic ultrasound as a monitoring tool in the intensive care unit.  
372 *Annals of translational medicine* **2017**, *5*.
- 373 3. Laghi, F.; Tobin, M.J. Disorders of the respiratory muscles. *American journal of respiratory and critical care  
374 medicine* **2003**, *168*, 10–48.
- 375 4. Khan, A.; Morgenthaler, T.I.; Ramar, K. Sleep disordered breathing in isolated unilateral and bilateral  
376 diaphragmatic dysfunction. *Journal of clinical sleep medicine: JCSM: official publication of the American Academy  
377 of Sleep Medicine* **2014**, *10*, 509.
- 378 5. Heldt, G.P.; Ward III, R.J. Evaluation of Ultrasound-Based Sensor to Monitor Respiratory and  
379 Nonrespiratory Movement and Timing in Infants. *IEEE Trans. Biomed. Engineering* **2016**, *63*, 619–629.
- 380 6. Umbrello, M.; Formenti, P.; Longhi, D.; Galimberti, A.; Piva, I.; Pezzi, A.; Mistraletti, G.; Marini, J.J.;  
381 Iapichino, G. Diaphragm ultrasound as indicator of respiratory effort in critically ill patients undergoing  
382 assisted mechanical ventilation: a pilot clinical study. *Critical Care* **2015**, *19*, 161.
- 383 7. Javaheri, S.; Dempsey, J. Central sleep apnea. *Comprehensive Physiology* **2013**.
- 384 8. Sinharay, A.; Rakshit, R.; Khasnobish, A.; Chakravarty, T.; Ghosh, D.; Pal, A. The Ultrasonic Directional  
385 Tidal Breathing Pattern Sensor: Equitable Design Realization Based on Phase Information. *Sensors* **2017**,  
386 *17*, 1853.
- 387 9. Araujo, G.; Freire, R.; Silva, J.; Oliveira, A.; Jaguaribe, E. Breathing flow measurement with constant  
388 temperature hot-wire anemometer for forced oscillations technique. *Instrumentation and Measurement  
389 Technology Conference, 2004. IMTC 04. Proceedings of the 21st IEEE*. IEEE, 2004, Vol. 1, pp. 730–733.
- 390 10. Bai, Y.W.; Li, W.T.; Chen, Y.W. Design and implementation of an embedded monitor system for detection  
391 of a patient's breath by double webcams. *Medical Measurements and Applications Proceedings (MeMeA)*,  
392 *2010 IEEE International Workshop on*. IEEE, 2010, pp. 171–176.
- 393 11. Bu, N.; Ueno, N.; Fukuda, O. Monitoring of Respiration and Heartbeat during Sleep using  
394 a Flexible Piezoelectric Film Sensor and Empirical Mode Decomposition. *2007 29th Annual*

395 International Conference of the IEEE Engineering in Medicine and Biology Society, 2007, pp. 1362–1366.  
396 doi:10.1109/IEMBS.2007.4352551.

397 12. Loriga, G.; Taccini, N.; Rossi, D.D.; Paradiso, R. Textile Sensing Interfaces for Cardiopulmonary Signs  
398 Monitoring. 2005 IEEE Engineering in Medicine and Biology 27th Annual Conference, 2005, pp. 7349–7352.  
399 doi:10.1109/IEMBS.2005.1616209.

400 13. Fekr, A.R.; Radecka, K.; Zilic, Z. Design and evaluation of an intelligent remote tidal volume variability  
401 monitoring system in e-health applications. *IEEE journal of biomedical and health informatics* 2015,  
402 19, 1532–1548.

403 14. Arlotto, P.; Grimaldi, M.; Naeck, R.; Ginoux, J.M. An Ultrasonic Contactless Sensor for Breathing  
404 Monitoring. *Sensors* 2014, 14, 15371. doi:10.3390/s140815371.

405 15. Shahshahani, A.; Bhadra, S.; Zilic, Z. A Continuous Respiratory Monitoring System Using Ultrasound  
406 Piezo Transducer. Circuits and Systems (ISCAS), 2018 IEEE International Symposium on. IEEE, 2018, pp.  
407 1–4.

408 16. Fouzas, S.; Priftis, K.N.; Anthracopoulos, M.B. Pulse oximetry in pediatric practice. *Pediatrics* 2011,  
409 128, 740–752.

410 17. Sahni, R. Noninvasive monitoring by photoplethysmography. *Clinics in perinatology* 2012, 39, 573–583.

411 18. Landsverk, S.A.; Hoiseth, L.O.; Kvandal, P.; Hisdal, J.; Skare, O.; Kirkeboen, K.A. Poor agreement between  
412 respiratory variations in pulse oximetry photoplethysmographic waveform amplitude and pulse pressure  
413 in intensive care unit patients. *Anesthesiology: The Journal of the American Society of Anesthesiologists* 2008,  
414 109, 849–855.

415 19. Shelley, K.H.; Jablonka, D.H.; Awad, A.A.; Stout, R.G.; Rezkanna, H.; Silverman, D.G. What is the best  
416 site for measuring the effect of ventilation on the pulse oximeter waveform? *Anesthesia & Analgesia* 2006,  
417 103, 372–377.

418 20. Iyriboz, Y.; Powers, S.; Morrow, J.; Ayers, D.; Landry, G. Accuracy of pulse oximeters in estimating heart  
419 rate at rest and during exercise. *British journal of sports medicine* 1991, 25, 162–164.

420 21. Felblinger, J.; Boesch, C. Amplitude demodulation of the electrocardiogram signal (ECG) for respiration  
421 monitoring and compensation during MR examinations. *Magnetic resonance in medicine* 1997, 38, 129–136.

422 22. Moody, G.B.; Mark, R.G.; Zuccola, A.; Mantero, S. Derivation of respiratory signals from multi-lead ECGs.  
423 *Computers in cardiology* 1985, 12, 113–116.

424 23. Wang, F.T.; Chan, H.L.; Wang, C.L.; Jian, H.M.; Lin, S.H. Instantaneous respiratory estimation from thoracic  
425 impedance by empirical mode decomposition. *Sensors* 2015, 15, 16372–16387.

426 24. Pantelopoulos, A.; Bourbakis, N.G. A Survey on Wearable Sensor-Based Systems for Health Monitoring  
427 and Prognosis. *IEEE Transactions on Systems, Man, and Cybernetics, Part C (Applications and Reviews)* 2010,  
428 40, 1–12. doi:10.1109/TSMCC.2009.2032660.

429 25. Sweeney, D.A. Point-of-Care Ultrasound. *Critical Care Medicine* 2015, 43, e330.

430 26. Zambon, M.; Beccaria, P.; Matsuno, J.; Gemma, M.; Frati, E.; Colombo, S.; Cabrini, L.; Landoni, G.; Zangrillo,  
431 A. Mechanical ventilation and diaphragmatic atrophy in critically ill patients: an ultrasound study. *Critical  
432 care medicine* 2016, 44, 1347–1352.

433 27. Garcia, M.J.; Rodriguez, L.; Ares, M.; Griffin, B.P.; Klein, A.L.; Stewart, W.J.; Thomas, J.D. Myocardial  
434 wall velocity assessment by pulsed Doppler tissue imaging: Characteristic findings in normal subjects.  
435 *American Heart Journal* 1996, 132, 648 – 656. doi:https://doi.org/10.1016/S0002-8703(96)90251-3.

436 28. Tole, N.M.; Ostensen, H.; Organization, W.H.; others. Basic physics of ultrasonic imaging 2005.

437 29. Shung, K. *Diagnostic Ultrasound: Imaging and Blood Flow Measurements*; Wiley, 1998.

438 30. Langen, K.; Jones, D. Organ motion and its management. *International Journal of Radiation Oncology●  
439 Biology● Physics* 2001, 50, 265–278.

440 31. De, A.T.; Estenne, M. Functional anatomy of the respiratory muscles. *Clinics in chest medicine* 1988,  
441 9, 175–193.

442 32. Sarwal, A.; Walker, F.O.; Cartwright, M.S. Neuromuscular ultrasound for evaluation of the diaphragm.  
443 *Muscle & nerve* 2013, 47, 319–329.

444 33. McKenzie, D.; Gandevia, S.; Gorman, R.; Southon, F. Dynamic changes in the zone of apposition and  
445 diaphragm length during maximal respiratory efforts. *Thorax* 1994, 49, 634–638.

446 34. Wait, J.L.; Nahormek, P.A.; Yost, W.T.; Rochester, D.P. Diaphragmatic thickness-lung volume relationship  
447 in vivo. *Journal of Applied Physiology* 1989, 67, 1560–1568.

448 35. Zambon, M.; Cabrini, L.; Zangrillo, A. Diaphragmatic ultrasound in critically ill patients. In *Annual Update*  
449 *in Intensive Care and Emergency Medicine* 2013; Springer, 2013; pp. 427–438.

450 36. Food.; Administration, D.; others. Guidance for Industry and FDA Staff Information for Manufacturers  
451 Seeking Marketing Clearance of Diagnostic Ultrasound Systems and Transducers. *Silver Spring: US FDA*  
452 **2008**.

453 37. Shahshahani, A.; Nafchi, D.R.; Zilic, Z. Ultrasound sensors and its application in human heart rate  
454 monitoring. 2017 IEEE International Symposium on Circuits and Systems (ISCAS), 2017, pp. 1–4.  
455 doi:10.1109/ISCAS.2017.8050899.

456 38. Holland, A.E.; Goldfarb, J.W.; Edelman, R.R. Diaphragmatic and cardiac motion during suspended  
457 breathing: preliminary experience and implications for breath-hold MR imaging. *Radiology* **1998**,  
458 209, 483–489.